DOI: 10.1002/cphc.200800310

Kinetics of Helix-Handedness Inversion: Folding and Unfolding in Aromatic Amide Oligomers

Nicolas Delsuc,[a] Takahiro Kawanami,[b] Julien Lefeuvre,[a] Atsuomi Shundo,[b] Hirotaka Ihara,[b] Makoto Takafuji,*[b] and Ivan Huc*[a]

A series of helically folded oligoamides of 8-amino-2-quinoline carboxylic acid possessing 6, 7, 8, 9, 10 or 16 units are prepared following convergent synthetic schemes. The right-handed (P) and the left-handed (M) helical conformers of these oligomers undergo an exchange slow enough to allow their chromatographic separation on a chiral stationary phase. Thus, the M conformer is isolated for each of these oligomers and its slow racemization in hexane/$CHCl_3$ solutions is monitored at various temperatures using chiral HPLC. The kinetics of racemization at different temperatures in hexane/$CHCl_3$ (75:25 vol/vol) are fitted to a first order kinetic model to yield the kinetic constant and the Gibbs energy of activation for oligomers having 6, 7, 8, 9, 10 or 16 quinoline units. This energy gives the first quantitative measure of the exceptional stability of the helical conformers of an aromatic amide foldamer with respect to its partly unfolded conformations that occur between an M helix and a P helix. The trend of the Gibbs energy as a function of oligomer length suggests that helix-handedness inversion does not require a complete unfolding of a helical strand and may instead occur through the propagation of a local unfolding separating two segments of opposite handedness.

1. Introduction

A number of synthetic oligomers and polymers have been shown to adopt well-defined folded conformations in solution that mimic the conformations of biopolymers.[1] Interest in these foldamers stems from the prospect to mimic not only biopolymer structures, but also their functions, thereby paving the way to a wide range of applications. On a more fundamental level, foldamers also provide model systems and a broader perspective to view biopolymer folding. After 15 years of intense research on foldamers, a wide body of evidence shows that folding is not only associated with biopolymers, but also occurs for a diverse range of chemical backbones. Some foldamer backbones are termed biotic because they are related to biopolymers in terms of their chemical structure and in terms of the noncovalent interactions that stabilize their folded conformations. For example, aliphatic β-, γ-, and δ-peptides are related to α-peptides; and numerous synthetic base-modified or backbone-modified analogues of nucleic acids have been produced.[1] Other foldamers are termed abiotic because their structures and folding mechanisms are remote from those of biopolymers. Herein, we present an investigation of the kinetics and thermodynamics of folding of abiotic aromatic oligoamide foldamers (AOFs) derived from 8-amino-2-quinoline carboxylic acid.

AOFs may adopt a wide range of helical or linear conformations stabilized primarily by local conformational preferences at aryl-amide linkages.[2] When hydrogen-bond donors or acceptors are introduced on an aryl ring in a position adjacent to an amide function, a preferred conformation occurs at the aryl–amide linkage due to conjugation, intramolecular hydrogen bonding with the amide CO or NH moieties and electrostatic interactions. In the case of the oligoamides of 8-amino-2-quinolinecarboxylic acid, attractions and repulsions between the amide moiety and the endocyclic quinoline nitrogen result in a bent conformation that eventually turns into a compact helix (Figure 1). The helical structure has been extensively characterized in the solid state and in solution.[3] Its pitch equals the thickness of one aromatic ring, 3.5 Å, and the number of units per helical turn is almost exactly 2.5. Aromatic stacking within the helix obviously comes as an additional stabilization of the conformation, especially in protic solvents in which solvophobic effects are strong.[3d] In general, the AOFs' folded conformations tend to be particularly stable, and examples of misfolding in the solid state are rare.[4] In the specific case of oligoamides of 2-amino-quinolinecarboxylic acid, helix stability reaches spectacular levels. For example, the NMR spectrum of octamer **8** (Figure 1) shows no sign of unfolding at 120° in DMSO.[3a]

The high stability of the AOFs' conformations, such as the helix of **8**, makes these objects very useful as building blocks to construct large artificial folded architectures[5] or as reliable

[a] *Dr. N. Delsuc, J. Lefeuvre, Dr. I. Huc*
Institut Européen de Chimie et Biologie
Université de Bordeaux – CNRS UMR 5248
2 rue Escarpit, 33607 Pessac (France)
Fax: (+33) 540002219
E-mail: i.huc@iecb.u-bordeaux.fr

[b] *T. Kawanami, Dr. A. Shundo, Prof. H. Ihara, Prof. M. Takafuji*
Department Applied Chemistry and Biochemistry
Kumamoto University, 2-39-1 Kurokami, Kumamoto 860-8555 (Japan)
Fax: (+81) 96342 3663
E-mail: takafuji@chem.kumamoto-u.ac.jp

Supporting information for this article is available on the WWW under http://dx.doi.org/10.1002/cphc.200800310.

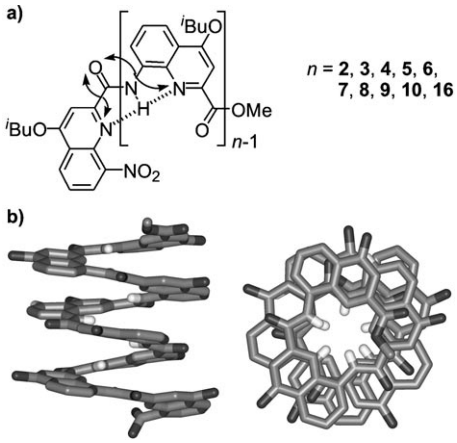

Figure 1. Structure of quinoline-derived oligoamide foldamers. a) Compounds considered in this manuscript are named according to the number of units in their sequence (e.g. for compound **5**, $n=5$). The formula shows hydrogen bonds (···) and electrostatic repulsions (↔) that stabilize the helically folded conformers; b) Side view (left) and top view (right) of the crystal structure of **8**.[3a] Isobutyl side chains and included solvent molecules are omitted for clarity.

scaffolds to interact with other substances.[6] In principle, the stability of a folded conformation is defined with respect to an unfolded state. For example, proteins are denaturated upon heating or in the presence of additives such as urea, and double- or triple-helical structures such as those of DNA or collagen display a melting temperature. However, in the case of the oligoamides of 8-amino-2-quinolinecarboxylic acid, no direct evidence of an unfolded conformation has been found and helix stability has only been addressed in qualitative terms. One may wonder whether an unfolded state of these objects exists or whether their conformational energy landscape is not simply a single well, that is, whether they qualify as *folded* structures. In fact, indirect evidence suggests that these structures are dynamic and that folding and unfolding do occur, albeit slowly, in solution. One piece of evidence is that molecules entrapped in the hollows of AOFs' helices are dynamically bonded and released.[6d,e] Further evidence is that helical conformations undergo a dynamic exchange between right-handed (P) and left-handed (M) helices and thus must transit through (partially) unfolded conformations.[5a,b,7] As shown herein, we now have determined the kinetics and Gibbs energy barriers of helix-handedness inversion for oligomers **6**–**10** and **16**. These barriers may be considered as a measure of helix stability, being the energy difference between a folded helix and the lowest-energy unfolded structure. The trend of the Gibbs energy as a function of oligomer length also provides insights into the actual nature of the unfolded intermediates and the mechanism of helix-handedness inversion.

2. Results and Discussion

2.1. Oligomer Synthesis and NMR Characterization

General methods for preparing quinoline-derived aromatic foldamers have already been reported, including **6**, **8**, **10** and the oligomers having 4 units or less.[3b,d] Oligomers **5**, **7**, **9** and **16** are new compounds prepared for the purpose of this study, following the general procedure (Scheme 1). Thus, pentamer **5**

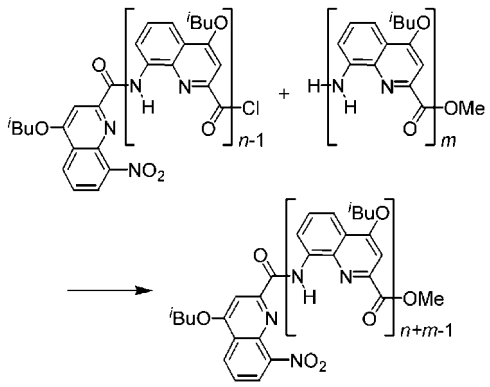

Scheme 1. Convergent synthetic strategy followed to prepare **2**–**10** and **16**.

is prepared from a monomer acid chloride and a tetramer amine ($n=1$, $m=4$), heptamer **7** from a tetramer acid chloride and a trimer amine ($n=4$, $m=3$), nonamer **9** from a tetramer acid chloride and a pentamer amine ($n=4$, $m=5$) and hexadecamer **16** from an octamer acid chloride and an octamer amine ($n=m=8$). All of these coupling reactions proceed smoothly in 60–80% yield, except for the formation of **16** which is produced at best in 25% yield, and the purification of which is troublesome. This low yield presumably arises from the steric hindrance associated with the large and stable helical conformation of both the amine nucleophile and acid chloride electrophile, which allow for side reactions such as anhydride formation[5c] to take place. This result corroborates the behaviors of other large AOFs[8] and one may have to resort to alternative synthetic strategies[9] to improve the yields.

Extensive characterization of the solid state and solution structures of these quinoline oligomers have already been reported.[3] A qualitative, yet compelling, illustration of the effect of folding on the local environment of the sequences is provided by the ^{1}H NMR spectra of **2**–**10** and **16** shown in Figure 2. Despite the repetitive nature of the sequences, the helical environment gives rise to different chemical shift values of one given proton on each monomer according to its position in the sequence, resulting in a remarkable spread of the ^{1}H NMR signals, even for **16**. A notable feature is the overall upfield shift of all signals upon increasing the length of the sequence. For instance, the signal of the methyl ester at the C-terminus is found at 2.93 ppm in **10** and at 2.83 ppm in **16**, despite the fact that the additional units are virtually introduced at the N-terminus, which is 14 Å away from the ester function. The amplitude of these upfield shifts are reminiscent of those observed in aromatic molecules in the solid state using magic-angle spinning ^{1}H NMR.[10] Assuming that ring current effects are considered as relatively short-ranged,[11] the actual origin of the chain-length dependence of chemical shift values in AOFs is not totally clear.[12] It might result from the cumulated addi-

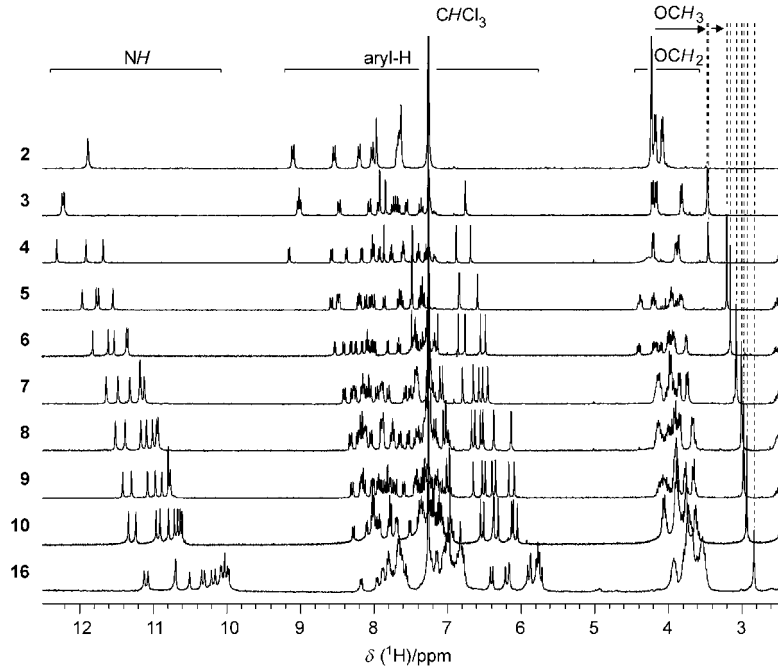

Figure 2. Part of the ^{1}H 300 or 400 MHz NMR spectra of **2**–**10** and **16** in $CDCl_3$. Compound numbering is defined in Figure 1.

tion of multiple weak ring current effects of distant quinoline rings that all stack perfectly aligned. It might also result from a progressive increase in helix stability with oligomer length that decreases local molecular motions and consequently enhances short-range ring current effects.

Another feature of the ^{1}H NMR spectra pointing to helical conformations that suggests an increase in helix stability as the oligomer length increases is the enantiotopic or diastereotopic aspect of the signals of the side chains' CH_2 units in the 3.4–4.4 ppm range. In **3** and **4**, these signals appear as (eventually broad) doublets, showing that the CH_2 protons are on average in the same environment despite the fact that they belong to an intrinsically chiral structure. Upon cooling, the signals of **4** become diastereotopic and split into doublets of doublets.[3b] These results are consistent with an equilibrium between the P and M helical conformation that is reached rapidly on the NMR timescale at room temperature, and slowly at low temperature. For all oligomers having 5 units or more, this exchange is slow at room temperature, resulting in diastereotopic patterns of the signals of CH_2 units. Thus, increasing oligomer length enhances the stability of the conformation. The extent of this stabilization appears to be significant because the diastereotopic signals do not coalesce upon heating for oligomers having 6 units or more at temperatures up to 100 °C. Furthermore, previous experiments showed that the helix-handedness inversion of analogues of **8** has a half-life of about 2.5 h in chloroform solution at room temperature,[7] and that the diastereomeric P and M helices of an octamer bearing a chiral residue can actually be separated by standard chromatography on silicagel, and their exchange subsequently monitored.[7b] We thus infer that the enantiomeric helices of various oligomers may be separated using chromatography on a chiral stationary phase and their racemization studied in a systematic way.

2.2. Chiral Separation and Kinetics of Helix-Handedness Inversion

Compounds **5**, **6**, **8** and **16** were used to optimize conditions for chromatographic chiral separations (Figure 3). The P and M helical conformers were well-separated on a Chiralpack stationary phase eluting with n-hexane/chloroform (75:25, v/v) at various eluent temperatures, provided that racemization remains insignificant at the timescale of chromatography, in this case 10–15 min. Chromatograms recorded using a circular dichroism (CD) detector at 385 nm show

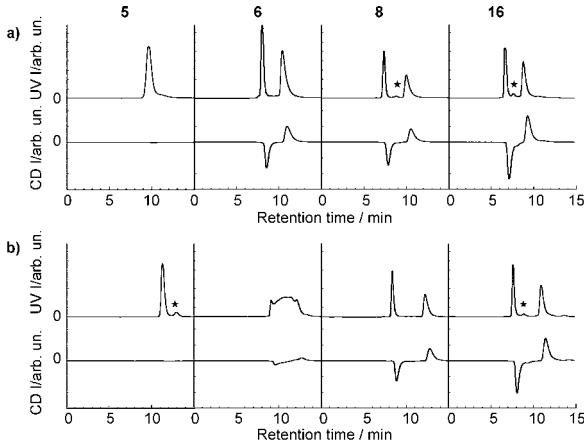

Figure 3. Chromatograms of **5**, **6**, **8**, and **16** on a chiral stationary phase recorded at a column temperature of a) 0 °C and b) 30 °C. For each chromatogram, the UV/Vis absorption at 350 nm (top trace) and the CD at 385 nm (bottom trace) are shown. Working conditions: Chiralpack IA column; eluent: *n*-hexane/chloroform (75:25, v/v); flow rate: 0.5 mL min^{-1}. Stars indicate the presence of impurities. The peaks of the UV traces show identical integration values within less than 2%.

one negative peak and one positive peak as expected for helices of opposite handedness. This allows one to attribute the peak with the smaller retention coefficient to the M helix (negative at 385 nm) and the other to the P helix (positive at 385 nm), based on a previous unambiguous absolute assignment of the helical handedness of these compounds.[7] The chromatographic parameters for **5**, **6**, **8** and **16** are shown in Table 1. Separation factors range from 3 to 8. Resolution factors typically range from 3 to 5 and tend to increase at higher temperature. These values are comparable to those measured

Table 1. Chromatographic parameters of **5**, **6**, **8**, and **16** at various temperatures.[a]

Temperature [°C]	**5**				**6**				**8**				**16**			
	t_M[b]	t_P[c]	α[d]	R[e]	t_M[b]	t_P[c]	α[d]	R[e]	t_M[b]	t_P[c]	α[d]	R[e]	t_M[b]	t_P[c]	α[d]	R[e]
0	9.63	9.63	1	0	7.99	10.39	2.7	2.9	7.35	9.97	4.5	3.3	6.60	8.73	7.9	3.1
10	10.31	10.31	1	0	8.43	11.09	2.4	3.4	7.69	10.83	3.8	4.1	6.96	9.55	7.6	3.8
20	10.89	10.89	1	0	8.77	11.71	–	–	8.04	11.65	3.4	4.4	7.28	10.32	5.0	4.5
30	11.28	11.28	1	0	9.09	12.08	–	–	8.35	12.20	3.0	5.3	7.54	10.89	4.1	4.7

[a] Conditions are the same as those in Figure 3. [b] Retention time (min) of the M helix. [c] Retention time (min) of the P helix. [d] Separation factors between M and P helices. [e] Resolution factors between the two helices.

for poly(quinoxaline-2,3-diyl)s[13], but are much higher than generally observed for helicenes on various chiral stationary phases,[14] for helical polymethacrylates[15] and poly-isocyanides,[16] and for isotactic chloral oligomers.[17a] In the case of pentamer **5**, no separation was achieved and a single peak is observed, indicating that the P and M helices equilibrate rapidly on the chromatographic timescale. For hexamer **6**, exchange between P and M helices is limited and separation can be achieved at column temperatures below 10 °C. At 20 °C and above, racemization occurs partially during the course of chromatography, and separation is not achieved. A characteristic peak cluster is observed instead (Figure 3 b, compound **6**) with two sharp peaks of nonconverted helices flanking a plateau formed by the species that underwent at least one interconversion event.

The chromatographic separation of M and P helices was achieved for all compounds **6**–**10** and **16**, using a CHIRALPAK 1A column with *n*-hexane/$CHCl_3$ (75:25 vol/vol) as the mobile phase. In each case, the first eluting fraction corresponding to the M helix was collected and allowed to stand at 0 °C, at 10 °C and at 30 °C. Racemization of these samples in *n*-hexane/$CHCl_3$ (75:25 vol/vol) was monitored, again using chiral analytical HPLC at regular time intervals, but at a column temperature of −5 °C to ensure that no further racemization takes place during chromatographic analysis. An example of the consecutive chromatograms recorded upon the racemization of **8** at 10 °C is shown in Figure 4 to illustrate the progressive appearance of the P helix. Only for the shorter oligomer **6** at a higher incubation temperature of 30 °C is racemization too fast to be monitored by this technique because it occurs during separation. In all other cases, racemization is conveniently monitored to give the time courses shown in Figure 5. These data are fitted to a simple first-order kinetic model (single exponential decay)[15] with excellent correlation coefficients ($r^2 = 0.993$–0.999) to yield apparent kinetic constants and half-lives of racemization defined as the time required for the pure M helix to reach 50 % enantiomeric excess (Table 2).

When comparing the racemization of the various oligomers at different temperatures, the most striking feature is the considerable difference between the fastest and the slowest processes. The half-life of racemization of **6** at 10 °C is about 12 min, and it is estimated to be over a year for **16** at 0 °C. Though the helix of **16** remains dynamic, kinetic inertness might arise at lower temperatures or for longer sequences. This spectacular stability illustrates the strength and coopera-

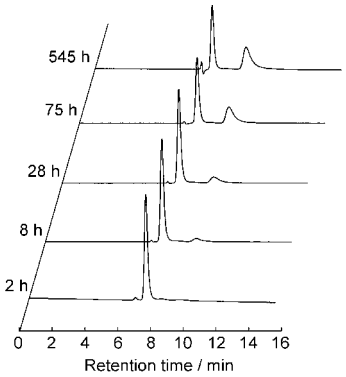

Figure 4. Time course of the racemization of **8** incubated in *n*-hexane/$CHCl_3$ (75:25 vol/vol) at 10 °C monitored by chiral chromatography. Conditions are those of Figure 3, except the column temperature (−5 °C). The peak at 6.5 min corresponds to the dead volume, and not to an impurity. It is due to the injection shock of the solvent, because the injected sample and mobile phase have slightly different compositions. The intensity of this peak may vary without following any trend.

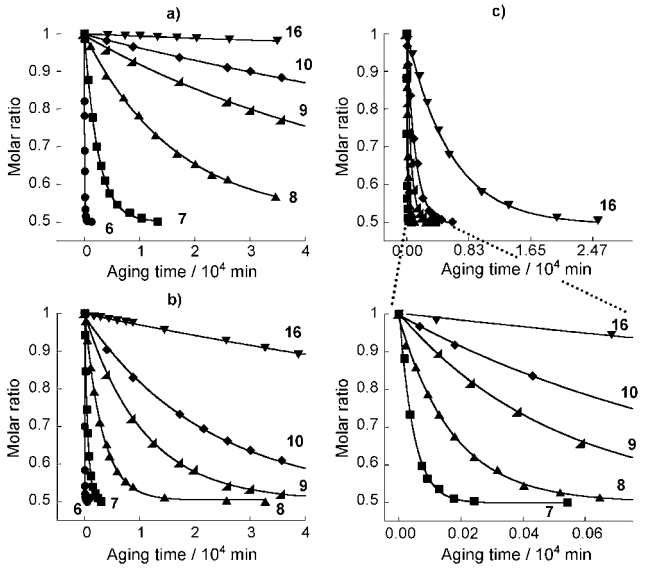

Figure 5. Time courses of the M-helix/P-helix molar ratio after isolation of the pure M helix as monitored by chiral HPLC for **6** (●), **7** (■), **8** (▲), **9** (◀), **10** (◆), and **16** (▼). Incubation solvent is *n*-hexane/chloroform (75/25, vol/vol) at a) 0 °C, b) 10 °C and c) 30 °C. HPLC conditions are the same as for Figure 3, except the column temperature (−5 °C). The lines are single exponential curve fittings.

Table 2. Kinetic and thermodynamic parameters of helix-handedness inversion for **6**–**10** and **16** at 0 °C, 10 °C and 30 °C, in *n*-hexane/chloroform (75:25 v/v).

n[a]	n_t[b]	T [°C]	k_{rac} [s^{-1}][c]	$t_{1/2}$ [h][d]	$\Delta G^{\neq}$ [kJ mol^{-1}][e]	$\Delta G^{\neq}/(n-1)$ [kJ mol^{-1}]
		0	1.3×10^{-4}	0.7	87.0	17.4
6	2.4	10	6.6×10^{-4}	0.2	86.4	17.3
		30	_[f]	_[f]	_[f]	_[f]
		0	3.3×10^{-6}	28.8	95.3	15.9
7	2.8	10	1.5×10^{-5}	6.3	95.3	15.9
		30	1.6×10^{-4}	0.5	95.7	16.0
		0	4.9×10^{-7}	196.4	99.6	14.2
8	3.2	10	2.6×10^{-6}	37.4	99.5	14.2
		30	4.6×10^{-5}	2.0	99.3	14.2
		0	1.4×10^{-7}	684.8	102.5	12.8
9	3.6	10	7.7×10^{-7}	125.0	102.3	12.8
		30	1.5×10^{-5}	6.4	102.2	12.8
		0	6.3×10^{-8}	1540.0	104.3	11.6
10	4	10	3.7×10^{-7}	262.5	104.1	11.6
		30	7.4×10^{-6}	13.1	104.0	11.5
		0	10×10^{-9}[g]	10000[g]	108.6	7.2
16	6.4	10	5.1×10^{-8}	1870.0	108.7	7.2
		30	1.5×10^{-6}	66.3	108.1	7.2

[a] Number of quinoline units in the sequence. [b] Number of helical turns. [c] Apparent first order rate constant of helix-handedness inversion. [d] Half-life of helix-handedness inversion. [e] Gibbs energy of activation. [f] Too fast to be measured. [g] These values are estimated based on a partial racemization, the process being too slow to be monitored to completion.

methacrylate),[15a] poly-isocyanides,[16,19b] and in some poly-acetylenes.[20] Energy barriers of 67 and 82 kJ mol^{-1} have been recorded in pentameric and hexameric isotactic chloral oligomers,[17] and barriers are in the 90–180 kJ mol^{-1} range for [5,6,7,8,9]-helicenes.[21] In all these examples, high energy barriers arise from a strong local steric hindrance of rotation about each sigma bond of the oligomer or polymer backbone or, in the case of helicenes, from the absence of bonds in the backbone able to rotate. In contrast, rotation about sigma bonds in compounds **2**–**16** is not subject to local steric hindrance. Barriers of rotation about sigma bonds are nevertheless high because of π-conjugation and local electrostatic attractions and repulsions. Additionally, hindrance occurs indirectly in the compact helical conformations—in other words, intramolecular aromatic stacking has to be disrupted to allow an unhindered rotation about sigma bonds. The outcome is that kinetics of helix-handedness inversion of AOFs are comparable to those of rigid helical structures. They differ much from those of α- or 3_{10}- peptidic helices for which handedness inversion is fast on the NMR timescale, that is, in the 100 ms regime or less, unless external stabilization is brought about by covalent crosslinks.[22]

tivity of the forces responsible for the folding in AOFs in general and of oligoamides of 8-quinoline-2-carboxylic acid in particular. The strong increase in helix stability when oligomer length increases suggests some cooperative effects among the forces involved. The influence of temperature is also remarkable, as illustrated by the time course of the racemization of **16** at 0 °C (Figure 5a, half-life > 1 year) and at 30 °C (Figure 5c, half-life < 3 days).

From the values of the kinetic constants of helix-handedness inversion at various temperatures, we use the Eyring equation (Experimetal Section) to extract the Gibbs energy barrier of activation between M and P helices (Table 2 and Figure 7).[18] The Gibbs energies are again very large, ranging from 87 kJ mol^{-1} for **6** to over 108 kJ mol^{-1} for **16**. They represent the energy difference between the folded helix and a transition state through which the oligomer must pass to undergo helical handedness inversion. This transition state is defined by the rate limiting pathway. Though of unknown structure, it is necessarily partly unfolded and, on average, achiral. In this respect, the Gibbs energy values provide the first quantitative measure of the energy required to unfold a helix partially and thus of the stability of the helical conformations of these compounds.

To provide a better perspective on these energy barriers of helix-handedness inversion, they should be compared to the values measured with other oligomers and polymers, taking into account the forces involved in stabilizing helical conformations in each case.[19] For example, energy barriers of helix-handedness inversion ranging from 100–133 kJ mol^{-1} have been measured in quinoxaline pentamers and hexamers; handedness inversion is even kinetically inert when oligomers are terminated by an appropriate chiral palladium complex.[13] Kinetic inertness is also reached in helical poly(triphenylmethyl

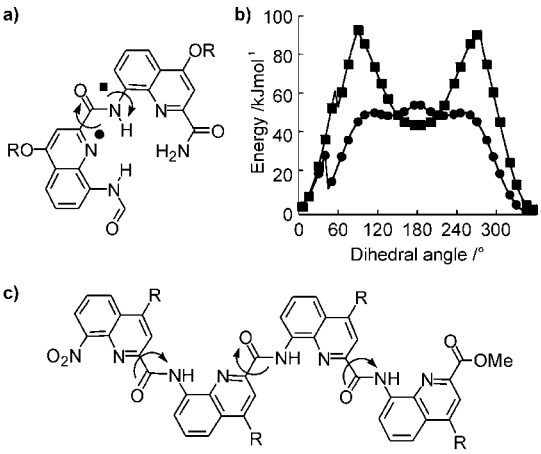

Figure 6. a) The structure of the molecular model used for the MM-calculation of the torsion energies for quinoline–NHCO (■) and quinoline–CONH (●) linkages. b) The torsion energies for quinoline–NHCO and quinoline–CONH linkages. c) An unfolded ribbon-like tetramer. The calculations are performed using the MMFFs force field and TNCG algorithm in Macromodel.[23]

2.3. Mechanism of Helix-Handedness Inversion

Helix-handedness inversion can only be achieved through rotations about aryl-amide bonds, that is, through the disruption of a local conformation preference and of interactions associated with aromatic stacking. We performed molecular mechanics calculations to estimate the energy barrier of rotations about aryl-CONH and aryl-NHCO linkages. As shown in Figure 6, these two rotations show quite different energy profiles. The barrier of rotation about the aryl-NHCO is considerably higher than that of the aryl-CONH, but this rotation also features a local minimum at 180°, apparently due to an attractive interaction between the rotated amide CO in position 8 and the amide NH in position 2. When an aryl-amide bond rotation is to take place within an oligomer, the barrier becomes even higher due to the hindrance that arises from aryl groups above and below the site where rotation takes place—in other words because aryl–aryl interactions must be disrupted to allow rotation.

For **6**–**10** and **16**, a plausible intermediate between the M and the P helices is a completely unfolded, achiral, ribbon-like conformation (Figure 6c). The examination of molecular models shows that to reach such an unfolded conformation with no intramolecular aryl–aryl overlap, a 180° aryl–amide rotation—either aryl–CONH or aryl–NHCO—must occur at every amide bond. The energy associated with each of these rotations includes the torsion energy of the aryl amide bond (Figure 6b) and also the energy to disrupt intramolecular π–π stacking associated with the quinoline that is being rotated. This is a constant term for all rotations, except for the last two. For them little or no intramolecular π–π stacking is involved. Thus, if the model of complete unfolding is valid, then the global energy barrier of helix-handedness inversion would be expected to increase essentially linearly with the number of amide linkages in the sequence. However, as shown in Table 2 and Figure 7, the actual trend is quite different, and the Gibbs

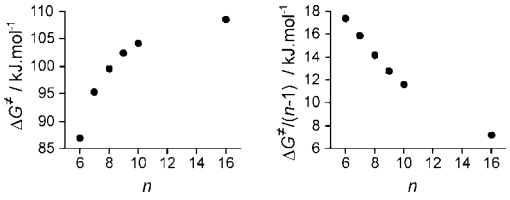

Figure 7. Trend of the Gibbs energy of helix-handedness inversion (left), and of the Gibbs energy of helix-handedness inversion per amide bond (right) as a function of the number of quinoline units in the oligomer (see also Table 2).

energy of activation per amide bond steadily decreases from the hexamer (17.4 kJ mol^{-1}) to hexadecamer (7.2 kJ mol^{-1}). Thus, one must assume that helix-handedness inversion does not occur through a complete unfolding of the helical strand.

As an alternative mechanism, one may propose that a local unfolding—that is, a local 180° rotation about a few aryl amide bonds—separating two helical segments of opposite handedness might propagate along the strand and result in complete handedness inversion. The molecular models shown in Figure 8 illustrate such a mechanism for hexadecamer **16**. These models show that partly unfolded conformations correspond to local, probably shallow, energy minima. They suggest that as few as two 180° rotations at consecutive aryl-amide linkages may constitute a local center of inversion of helix handedness that may propagate along the strand through some sort of hopping mechanism to allow the conversion of a P helix into an M helix, as has been proposed for helical polymers with low inversion barriers such as poly-isocyanates[24] and for pyridine–pyrimidine oligomers.[25] It seems likely that such a hopping mechanism would start from a helix end and not from its center, because fewer stacking interactions have to be broken at once upon unfolding one or two terminal quinoline units.

3. Conclusions

The kinetic and thermodynamic parameters associated with the folding and unfolding of an oligomer or polymer vary greatly depending on its size, chemical nature and the forces involved in stabilizing the folded conformation. Consequently, the measure of conformational stability comes in various formats. For helical α-peptides, a percentage of helical content based on circular dichroism is often proposed. For multiple helices such as those of nucleic acids and collagen, a melting temperature can be measured. In the case of AOFs, the absence of measurable amounts of unfolded conformers and the lack of information about their possible structure makes it difficult to assess conformational stability. The only (partly) unfolded conformers whose existence is obvious are the intermediate structures between P and M conformations. We have thus proposed to use the energy difference between these intermediates and the folded helix, namely, the energy barrier of helix-handedness interconversion, as a measure of conformation stability.

Thanks to the successful chromatographic separation of the P and M conformers of quinoline-based AOFs of various lengths, we have been able to assess the kinetic and thermodynamic parameters of helix-handedness inversion. These data provide a sound illustration of the high stability of these helical structures. However, even the longest oligomers still show a measurable, albeit slow, racemization. Their structures remain dynamic over long time scales and true kinetic inertness is not reached. Nevertheless, it appears that the features of helical AOFs somewhat relate to those of some sterically hindered or rigid helical molecules such as helicenes, poly(quinoxaline-2,3-diyl)s, poly(triphenylmethyl methacrylate), or isotactic chloral oligomers in terms of helix stability whilst they may relate to polymers with lower inversion barrier in terms of their possible helix-handedness inversion mechanism.

Experimental Section

HPLC and kinetic measurements: HPLC separations were performed by using a stainless-steel CHIRALPAK IA column (250 mm × 4.6 mm I.D., 5 μm particle-size) [Daicel Chemical Industries, Ltd.,

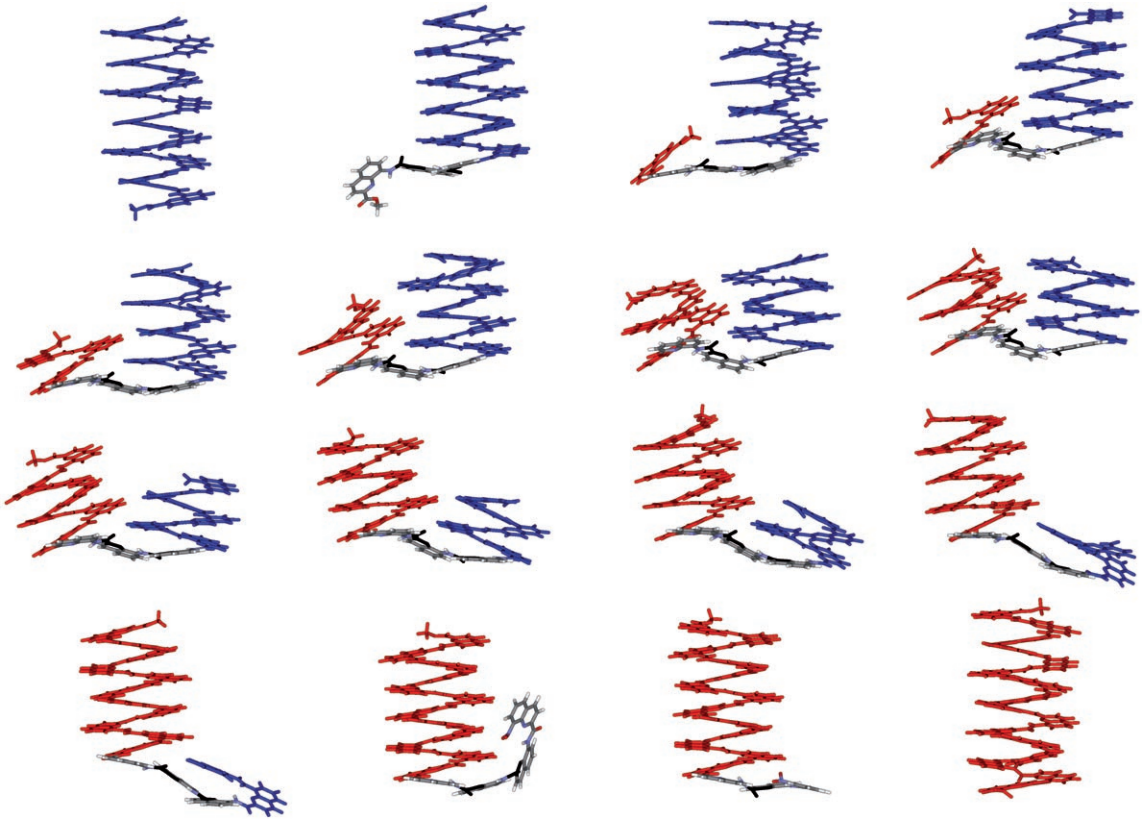

Figure 8. Energy-minimized conformations (MMFFs force field and TNCG algorithm in Macromodel.[23]) of hexadecamer **16** in which 180° rotations have been performed about two consecutive aryl-CONH linkages, resulting in a stretch of three consecutive unfolded quinoline units shown in grey. A right-handed (blue) and a left-handed (red) helical segment are properly folded on either side of the stretch of unfolded units, suggesting that this local unfolding might propagate from one end of the helix to the other.

Tokyo, Japan]. HPLC-grade solvents were supplied by Nacalai Tesque, Inc. (Kyoto, Japan). The HPLC system consisted of a JASCO 980 (JASCO, Tokyo, Japan) pump equipped with a Rheodyne injector (Rohnert Park, CA, USA), a 20-µl sample loop and a JASCO column jacket. The chromatograms were detected with a JASCO Model CD 2095 Plus chiral detector and JASCO Model MD2010 multiwavelength UV detector. Chiral separation of the oligomer was carried out with a *n*-hexane/chloroform (75:25 v/v) mixture as a mobile phase (flow rate: 0.5 mL min^{-1}, temperature: $-5\,^{\circ}$C). This ratio provided optimal separation. The initial stock solutions were prepared in a *n*-hexane/chloroform mixture 5:3 v/v, in which the oligomers are more soluble than in the eluting solvent. The racemic oligomer was dissolved in this solvent mixture and the solution was injected into HPLC. The fraction of left-handed helical conformer (M) was collected and aged at a given temperature directly in the eluting solvent (*n*-hexane/chloroform 75:25 vol:vol). The appearance of the P conformer was monitored under the above-mentioned HPLC conditions. The value of chromatographic monitoring over other techniques such as circular dichroism should be pointed to. Though not as fast to implement, HPLC is particularly reliable for the slowest kinetics because the proportions between P and M helices can be measured directly. The data are thus not sensitive to effects such as slow evaporation or calibration of the spectrometers.

The racemization rate constant (k_{rac}) of each oligomer was obtained by curve fitting to an exponential equation [Eq. (1)]:

$$\frac{[M]}{[M]_0} = \frac{1}{2}e^{[-2k(rac)t]} + \frac{1}{2} \quad (1)$$

where t is the aging time. Half-lives ($t_{1/2}$) were calculated following Equation (2):

$$t_{1/2} = -\frac{\ln(1/2)}{2k_{rac}} \quad (2)$$

The kinetic and thermodynamic parameters of helix-handedness inversion for oligomers were calculated using the Eyring equation [Eq. (3)]:[18]

$$\Delta G^{\neq} = -RT\ln\left(\frac{k_{rac}h}{k_b T}\right) \quad (3)$$

where R is the gas constant, h is Plank's constant and k_b is the Boltzmann constant.

Synthetic procedures: Unless otherwise stated, materials were obtained from commercial suppliers and used without further purification. CH_2Cl_2 and diisopropylethylamine (DIEA) were distilled from CaH_2 prior to use. Chemical shifts are reported in ppm and are calibrated against residual solvent signal of $CDCl_3$ ($\delta = 7.26$, 77.0). All coupling constants are reported in Hz. Silica gel chromatography was performed using Merck Kieselgel Si 60. Electronic impact mass spectra were obtained in the positive ion mode and matrix-assisted laser desorption ionization time-of-flight (MALDI) mass spectra

were obtained in positive-ion mode using α-cyanohydroxycinnamic acid as a matrix.

General procedure for acylation reactions (Scheme 1): The acid chloride (1 equiv) dissolved in dry CH_2Cl_2 (DCM) at 0 °C was added via cannula to a solution of the amine (1 equiv) in dry CH_2Cl_2 at 0 °C containing DIEA (5.5 equiv) under an inert atmosphere. The reaction mixture was stirred overnight at room temperature, whereafter the solvent was evaporated. The product was purified by silica gel chromatography using a gradient from 98:2 to 90:10 toluene/EtOAc v/v to yield the product as a yellow solid.

Pentamer **5** was sythesized from the tetramer amine[3b] (200 mg, 0.2 mmol, 1 equiv), DIEA (190 μL, 1.1 mmol, 5.5 equiv) in DCM (3 mL), and the monomer acid chloride[3b] (62 mg, 0.2 mmol, 1 equiv) in DCM (2 mL). Yield: 182 mg (72%). ^{1}H NMR (300 MHz, $CDCl_3$): δ = 11.96 (1H, s), 11.77 (1H, s), 11.74 (1H, s), 11.55 (1H, s), 8.58 (1H, dd, J = 8.4 Hz, J = 2.0 Hz), 8.48 (2H, dd, J = 7.8 Hz, J = 1.5 Hz), 8.20 (2H, m), 8.12–8.00 (3H, m), 7.86 (1H, d, J = 7.5 Hz), 7.68–7.60 (2H, m), 7.48 (3H, s), 7.39–7.31 (3H, m), 6.84 (1H, s), 6.83 (1H, s), 6.60 (1H, s), 4.39 (2H, m), 4.20 (2H, m), 3.98–3.81 (6H, m), 2.57–2.25 (5H, m), 1.32–1.14 ppm (30H, m). ^{13}C NMR (75 MHz, $CDCl_3$): δ = 163.7, 163.2, 163.0, 162.9, 162.8, 162.1, 161.9, 161.1, 160.7, 160.4, 153.4, 150.4, 149.1, 149.0, 145.1, 145.0, 138.9, 138.8, 138.3, 138.2, 137.9, 134.2, 133.9, 133.6, 127.7, 127.4, 127.1, 126.6, 126.4, 125.6, 124.0, 123.8, 122.3, 121.9, 121.7, 121.6, 117.0, 116.8, 116.5, 116.3, 116.2, 116.1, 115.2, 100.2, 99.6, 97.9, 97.0, 75.6, 75.3, 75.2, 75.1, 74.8, 51.8, 28.2, 28.1, 28.0, 19.3, 19.2, 19.1 ppm. MS (ESI+): m/z = 1273.5 $[M+H]^+$, 1295.5 $[M+Na]^+$.

Heptamer **7**, sythesized from the tetramer acid chloride[3b] (112 mg, 0.11 mmol, 1 equiv) and DIEA (103 μL, 0.55 mmol, 5.5 equiv) in DCM (2 mL) and the trimer amine (99 mg, 0.11 mmol, 1 equiv) in DCM (3 mL) Yield: 182 mg (66%). ^{1}H NMR (300 MHz, $CDCl_3$): δ = 11.64 (1H, s), 11.48 (1H, s), 11.31 (1H, s), 11.18 (2H, s), 11.12 (1H, s), 8.40 (1H, d, J = 8.1 Hz), 8.29 (1H, d, J = 7.6 Hz), 8.26 (1H, d, J = 7.6 Hz), 8.15 (2H, m), 8.07 (2H, m), 7.96 (1H, d, J = 8.3 Hz), 7.91 (1H, d, J = 7.9 Hz), 7.89 (1H, d, J = 7.9 Hz), 7.80 (1H, d, J = 8.3 Hz), 7.58 (1H, d, J = 7.6 Hz), 7.51 (1H, d, J = 7.4 Hz), 7.47–7.40 (6H, m), 7.2 (2H, m), 7.11 (1H, s), 7.07 (1H, s), 6.65 (1H, s), 6.58 (1H, s), 6.52 (1H, s), 6.80 (1H, s), 6.46 (1H, s), 4.19–4.10 (4H, m), 4.04–3.84 (8H, m), 3.74 (2H, d, J = 6.2 Hz), 3.08 (3H, s), 2.55–2.23 (7H, m), 1.37–1.15 ppm (42H, m). ^{13}C NMR (100 MHz, $CDCl_3$): δ = 163.6, 162.8, 162.7, 162.5, 161.9, 161.2, 160.8, 160.5, 160.1, 160.0, 159.2, 152.9, 149.8, 149.1, 149.0, 148.8, 148.7, 145.1, 144.7, 138.7, 138.3, 138.0, 137.7, 137.5, 134.2, 133.5, 133.4, 132.7, 127.9, 127.4, 126.9, 126.6, 126.3, 125.9, 125.7, 125.5, 123.8, 123.6, 122.5, 122.3, 121.6, 121.5, 121.4, 117.1, 116.7, 116.6, 116.4, 116.2, 116.1, 116.0, 115.8, 100.0, 99.8, 99.4, 98.8, 98.3, 97.6, 97.5, 75.5, 75.3, 75.2, 74.9, 74.7, 51.9, 28.1, 28.0, 19.5, 19.4, 19.3, 19.2, 19.1 ppm. MS (maldi): m/z = 1757.55 $[M+H]^+$, 1779.51 $[M+Na]^+$, 1795.54 $[M+K]^+$.

Nonamer **9**, from the tetramer acid chloride[3b] (82 mg, 0.08 mmol, 1 equiv) and DIEA (75 μL, 0.43 mmol, 5.5 equiv) in DCM (1.8 mL) and the pentamer amine (98 mg, 0.08 mmol, 1 equiv) in DCM (2 mL). Yield: 106 mg (60% yields). ^{1}H NMR (300 MHz, $CDCl_3$): δ = 11.41 (1H, s), 11.29 (1H, s), 11.08 (1H, s), 11.00 (1H, s), 10.88 (1H, s), 10.79 (2H, s), 10.77 (1H, s), 8.29 (1H, d, J = 8.1 Hz), 8.19–8.12 (3H, m), 8.04–8.00 (2H, m), 7.96–7.69 (6H, m), 7.59 (1H, d, J = 7.6 Hz), 7.46–6.95 (20H, m), 6.65 (1H, s), 6.53 (1H, s), 6.49 (1H, s), 6.40 (1H, s), 6.35 (1H, s), 6.17 (1H, s), 6.10 (1H, s), 4.16–3.62 (18H, m), 2.98 (3H, s), 2.58–2.14 (9H, m), 1.38–1.09 ppm (54H, m). ^{13}C NMR (75 MHz, $CDCl_3$): δ = 163.6, 162.6, 162.5, 162.4, 162.3, 162.2, 161.8, 160.9, 160.6, 160.4, 159.9, 159.6, 159.2, 159.0, 152.9, 149.8, 148.9, 148.7, 148.5, 148.4, 148.1, 144.9, 144.5, 138.5, 137.9, 137.8, 137.5, 137.2, 134.0, 133.4, 133.1, 132.8, 132.6, 132.3, 127.8, 127.3, 126.7, 126.1, 125.8, 125.6, 125.5, 125.3, 123.6, 123.4, 122.4, 122.2, 122.1, 121.8, 121.4, 121.3, 121.2, 117.1, 116.9, 116.7, 116.6, 116.4, 116.1, 116.0, 115.9, 115.7, 115.6, 115.4, 99.9, 99.7, 99.4, 98.8, 98.6, 98.4, 97.8, 97.4, 97.3, 75.4, 75.2, 75.0, 74.9, 74.8, 74.6, 51.8, 28.1, 28.0, 27.9, 19.5, 19.4, 19.3, 19.2, 19.1 ppm. MS (maldi): m/z = 2241.6 $[M+H]^+$, 2279.6 $[M+K]^+$.

Hexadecamer **16**, sythesized from the octamer acid chloride[3b] (60 mg, 0.03 mmol, 1 equiv) and DIEA (29 μL, 0.14 mmol, 5.5 equiv) in DCM (0.8 mL) and the octamer amine[3b] (59 mg, 0.03 mmol, 1 equiv) in DCM (1 mL). Yeild: 20 mg (24%). ^{1}H NMR (400 MHz, $CDCl_3$): δ = 11.12 (1H, s), 11.06 (1H, s), 10.69 (2H, s), 10.50 (1H, s), 10.34 (1H, s), 10.30 (1H, s), 10.21 (1H, s), 10.15 (1H, s), 10.09 (1H, s), 10.07 (1H, s), 10.03 (2H, s), 9.99 (1H, s), 9.97 (1H, s), 8.17 (1H, d, J = 7.6 Hz), 7.97 (1H, d, J = 7.1 Hz), 7.89–7.55 (15H, m), 7.23–6.75 (31H, m), 6.42 (1H, s), 6.38 (1H, s), 6.21 (1H, s), 6.17 (1H, s), 6.15 (1H, s), 5.91 (1H, s), 5.87 (2H, s), 5.79 (2H, s), 5.77 (3H, s), 5.75 (2H, s), 5.71 (1H, s), 3.92–3.40 (32H, m), 2.83 (3H, s), 2.28–2.07 (16H, m), 1.25–1.01 ppm (96H, m). MS (maldi) : m/z = 3936.5 $[M+H]^+$, 3958.5 $[M+Na]^+$.

Acknowledgements

This work was supported by an ANR grant (project no. NT05-3_44880), by the French Ministry of Research (predoctoral fellowship to N.D.).

Keywords: chiral resolution · chirality · chromatography · foldamers · helical structures

[1] *Foldamer. Structure, Properties and Applications* (Eds.: S. Hecht, I. Huc), Wiley-VCH, Weinheim, **2007**; C. M. Goodman, S. Choi, S. Shandler, W. F. DeGrado, *Nat. Chem. Biol.* **2007**, *3*, 252; D. J. Hill, M. J. Mio, R. B. Prince, T. S. Hughes, J. S. Moore, *Chem. Rev.* **2001**, *101*, 3893; S. H. Gellman, *Acc. Chem. Res.* **1998**, *31*, 173.

[2] Z.-T. Li, J.-L. Hou, C. Li, H.-P. Yi, *Chem. Asian J.* **2006**, *1*, 766; I. Huc, *Eur. J. Org. Chem.* **2004**, 17; B. Gong, *Chem. Eur. J.* **2001**, *7*, 4336; Z.-T. Li, J.-L. Hou, C. Li, *Acc. Chem. Res.* **2008**, DOI: 10.1021/ar700219m.

[3] a) H. Jiang, J.-M. Léger, I. Huc, *J. Am. Chem. Soc.* **2003**, *125*, 3448; b) H. Jiang, J.-M. Léger, C. Dolain, P. Guionneau, I. Huc, *Tetrahedron* **2003**, *59*, 8365; c) C. Dolain, A. Grélard, M. Laguerre, H. Jiang, V. Maurizot, I. Huc, *Chem. Eur. J.* **2005**, *11*, 6135; d) E. R. Gillies, C. Dolain, J.-M. Léger, I. Huc, *J. Org. Chem.* **2006**, *71*, 7931.

[4] Y. Hamuro, S. J. Geib, A. D. Hamilton, *J. Am. Chem. Soc.* **1996**, *118*, 7529; Y. Hamuro, S. J. Geib, A. D. Hamilton, *J. Am. Chem. Soc.* **1997**, *119*, 10587; E. Berni, B. Kauffmann, C. Bao, J. Lefeuvre, D. M. Bassani, I. Huc, *Chem. Eur. J.* **2007**, *13*, 8463.

[5] a) H.-Y. Hu, J.-F. Xiang, Y. Yang, C.-F. Chen, *Org. Lett.* **2008**, *10*, 69; b) N. Delsuc, J.-M. Léger, S. Massip, I. Huc, *Angew. Chem.* **2007**, *119*, 218; *Angew. Chem. Int. Ed.* **2007**, *46*, 214; c) C. Dolain, J.-M. Léger, N. Delsuc, H. Gornitzka, I. Huc, *Proc. Natl. Acad. Sci. USA* **2005**, *102*, 16146; d) V. Maurizot, C. Dolain, Y. Leydet, J.-M. Léger, P. Guionneau, I. Huc, *J. Am. Chem. Soc.* **2004**, *126*, 10049.

[6] a) For a review, see: J. Becerril, J. M. Rodriguez, I. Saraogi, A. D. Hamilton in *Foldamers: Structure, Properties and Applications* (Eds.: S. Hecht, I. Huc), Wiley-VCH, Weinheim, **2007**, pp. 195–228; b) J.-L. Hou, X.-B. Shao, G.-J. Chen, X.-Y. Zhou, X.-K. Jiang, Z.-T. Li, *J. Am. Chem. Soc.* **2004**, *126*, 12386; c) C. Li, G.-T. Wang, H.-P. Yi, X.-K. Jiang, Z.-T. Li, R.-X. Wang, *Org. Lett.* **2007**, *9*, 1797; d) J. Garric, J.-M. Léger, I. Huc, *Angew. Chem.* **2005**, *117*, 1990; *Angew. Chem. Int. Ed.* **2005**, *44*, 1954; e) J. Garric, J.-M. Léger, I. Huc, *Chem. Eur. J.* **2007**, *13*, 8454; f) D.-J. Feng, G.-T. Wang, J. Wu, R.-X. Wang, Z.-T. Li, *Tetrahedron Lett.* **2007**, *48*, 6181; g) J. Wu, F. Fang, W.-Y. Lu, J.-L. Hou, C. Li, Z.-Q. Wu, X.-K. Jiang, Z.-T. Li, Y.-H. Yu, *J. Org. Chem.* **2007**, *72*, 2897; h) Z.-Q. Wu, C.-Z. Li, D.-J. Feng, X.-K. Jiang, Z.-T. Li, *Tetra-*

hedron **2006**, *62*, 11 054; i) J. Zhu, J.-B. Lin, Y.-X. Xu, X.-B. Shao, X.-K. Jiang, Z.-T. Li, *J. Am. Chem. Soc.* **2006**, *128*, 12 307; j) Z.-Q. Wu, X.-B. Shao, C. Li, J.-L. Hou, K. Wang, X.-K. Jiang, Z.-T. Li, *J. Am. Chem. Soc.* **2005**, *127*, 17 460.

[7] a) H. Jiang, C. Dolain, J.- M. Léger, H. Gornitzka, I. Huc, *J. Am. Chem. Soc.* **2004**, *126*, 1034; b) C. Dolain, H. Jiang, J.-M. Léger, P. Guionneau, I. Huc, *J. Am. Chem. Soc.* **2005**, *127*, 12 943.

[8] B. Gong, H. Zeng, J. Zhu, L. Yuan, Y. Han, S. Cheng, M. Furukawa, R. D. Parra, A. Y. Kovalevsky, J. L. Mills, E. Skrzypczak-Jankun, S. Martinovic, R. D. Smith, C. Zheng, T. Szyperski, X. C. Zeng, *Proc. Natl. Acad. Sci. USA* **2002**, *99*, 11 583.

[9] A. Zhang, J. S. Ferguson, K. Yamato, C. Zheng, B. Gong, *Org. Lett.* **2006**, *8*, 5117.

[10] J. Schmidt, A. Hoffmann, H. W. Spiess, D. Sebastiani, *J. Phys. Chem. B* **2006**, *110*, 23 204.

[11] N. H. Martin, N. W. Allen III, J. C. Moore, *J. Mol. Graphics Modell.* **2000**, *18*, 242; M. B. Ferraro, P. Lazzeretti, R. G. Viglione, R. Zanasi, *Chem. Phys. Lett.* **2004**, *390*, 268.

[12] For interpreting chain length variation of a selected property, see: M. T. Stone, J. M. Heemstra, J. S. Moore, *Acc. Chem. Res.* **2006**, *39*, 11.

[13] Y. Ito, Y. Kojima, M. Murakami, M. Suginome, *Bull. Chem. Soc. Jpn.* **1997**, *70*, 2801.

[14] F. Mikeš, G. Boshart, E. Gil-Av, *J. Chem. Soc. Chem. Commun.* **1976**, 99; F. Mikeš, G. Boshart, *J. Chem. Soc. Chem. Commun.* **1978**, 173; Y. H. Kim, A. Tishbee, E. Gil-Av, *Science* **1981**, *213*, 1379; F. Furche, R. Ahlrichs, C. Wachsmann, E. Weber, A. Sobanski, F. Vögtle, S. Grimme, *J. Am. Chem. Soc.* **2000**, *122*, 1717.

[15] a) Y. Okamoto, I. Okamoto, H. J. Yuki, *Polym. Sci. Polym. Lett. Ed.* **1981**, *19*, 451; b) Y. Okamoto, H. Mohri, T. Nakano, K. Hatada, *J. Am. Chem. Soc.* **1989**, *111*, 5952.

[16] R. J. M. Nolte, A. J. M. Van Beijnen, W. Drenth, *J. Am. Chem. Soc.* **1974**, *96*, 5932; A. J. M. Van Beijnen, R. J. M. Nolte, W. Drenth, *Recl. Trav. Chim. Pays-Bas* **1980**, *99*, 121.

[17] a) K. Ute, K. Hirose, H. Kashimoto, H. Nakayama, K. Hatada, O. Vogl, *Polym. J.* **1993**, *25*, 1175; b) K. Ute, K. Hirose, H. Kashimoto, H. Nakayama, K. Hatada, *J. Am. Chem. Soc.* **1991**, *113*, 6305.

[18] J. Krupcik, P. Oswald, P. Májek, P. Sandra, D. W. Armstrong, *J. Chromatogr. A* **2003**, *1000*, 779; C. Danel, C. Foulon, J.-F. Goosens, J.-P. Bonte, C. Vaccher, *Tetrahedron: Asymmetry* **2006**, *17*, 2317.

[19] For reviews, see: a) E. Yashima, K. Maeda in *Foldamers: Structure, Properties and Applications* (Eds.: S. Hecht, I. Huc), Wiley-VCH, Weinheim, **2007**, pp. 331–366; b) M. B. J. Otten, G. A. Metselaar, J. J. L. M. Cornelissen, A. E. Rowan, R. J. M. Nolte in *Foldamers: Structure, Properties and Applications* (Eds.: S. Hecht, I. Huc), Wiley-VCH, Weinheim, **2007**, pp. 367–402.

[20] E. Yashima, K. Maeda, Y. Okamoto, *Nature* **1999**, *399*, 449; K. Maeda, K. Morino, Y. Okamoto, T. Sato, E. Yashima, *J. Am. Chem. Soc.* **2004**, *126*, 4329.

[21] a) [5]-Helicene: R. H. Martin, M. J. Marchant, *Tetrahedron Lett.* **1972**, *13*, 3707; b) [6,7,8,9]-helicenes: R. H. Martin, M. J. Marchant, *Tetrahedron* **1974**, *30*, 347; c) See also: O. Katzenelson, J. Edelstein, D. Avnir, *Tetrahedron: Asymmetry* **2000**, *11*, 2695.

[22] M. Kubasik, A. Brown, *ChemBioChem* **2005**, *6*, 1187; For a recent example of helix covalent crosslinking: N. Ousaka, T. Sato, R. Kuroda, *J. Am. Chem. Soc.* **2008**, *130*, 463.

[23] F. Mohamadi, N. G. J. Richards, W.-C. Guida, R. Liskamp, M. Lipton, C. Caufield, G. Chang, T. Hendrickson, W. C. Still, *J. Comput. Chem.* **1990**, *11*, 440. Standard parameters of the MMFFs force field were used. Though not optimized for aromatic amides, these parameters yield molecular models that very well reproduce solid-state X-ray structures. However, quantitative analysis of energy barriers may not be considered as very accurate.

[24] M. M. Green, J.-W. Park, T. Sato, A. Teramoto, S. Lifson, R. B. L. Selinger, J. Selinger, *Angew. Chem.* **1999**, *111*, 3328; *Angew. Chem. Int. Ed.* **1999**, *38*, 3138.

[25] M. Ohkita, J.-M. Lehn, G. Baum, D. Fenske, *Chem. Eur. J.* **1999**, *5*, 3471.

Received: May 23, 2008
Published online on ■■ ■■, 2008

ARTICLES

N. Delsuc, T. Kawanami, J. Lefeuvre, A. Shundo, H. Ihara, M. Takafuji, I. Huc**

■■ – ■■

Kinetics of Helix-Handedness Inversion: Folding and Unfolding in Aromatic Amide Oligomers

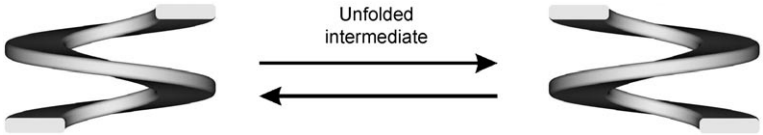

A measure of stability: Chiral resolution of helically folded aromatic amide oligomers allows the monitoring of their rates of racemization and, using the Eyring equation, to calculate the energy barriers between folded and transient unfolded states. Racemization most likely occurs through the gradual propagation of an inversion center between two helical segments of opposite handedness (see figure).

